

Attenuation of loop-receptor interactions with pseudoknot formation

Kirill A. Afonin¹, Yen-Ping Lin¹, Erin R. Calkins¹ and Luc Jaeger^{1,2,*}

¹Department of Chemistry and Biochemistry and ²Biomolecular Science and Engineering Program, University of California, Santa Barbara, CA 93106-9510, USA

Received September 3, 2011; Revised September 30, 2011; Accepted October 8, 2011

ABSTRACT

RNA tetraloops can recognize receptors to mediate long-range interactions in stable natural RNAs. *In vitro* selected GNRA tetraloop/receptor interactions are usually more ‘G/C-rich’ than their ‘A/U-rich’ natural counterparts. They are not as widespread in nature despite comparable biophysical and chemical properties. Moreover, while AA, AC and GU dinucleotide platforms occur in natural GAAA/11 nt receptors, the AA platform is somewhat preferred to the others. The apparent preference for ‘A/U-rich’ GNRA/receptor interactions in nature might stem from an evolutionary adaptation to avoid folding traps at the level of the larger molecular context. To provide evidences in favor of this hypothesis, several riboswitches based on natural and artificial GNRA receptors were investigated *in vitro* for their ability to prevent inter-molecular GNRA/receptor interactions by trapping the receptor sequence into an alternative intra-molecular pseudoknot. Extent of attenuation determined by native gel-shift assays and co-transcriptional assembly is correlated to the G/C content of the GNRA receptor. Our results shed light on the structural evolution of natural long-range interactions and provide design principles for RNA-based attenuator devices to be used in synthetic biology and RNA nanobiotechnology.

INTRODUCTION

In nature, long-range RNA interactions involving sequence positions often located hundreds of nucleotides away from each other, contribute to the folding of stable RNAs into functional three-dimensional (3D) structures (1,2). The most abundant of all identified long-range interactions are A-minor packing interactions, which occur

between stacked adenines and the shallow groove of small helical receptors composed of at least two Watson–Crick (WC) base pairs (bps) (3,4). In large ribozymes and riboswitches, A-minor interactions are often part of larger structural motifs involving GNRA tetraloops binding to helices or small receptors, with GYRA/helix and GAAA/11 nt receptor interactions being the most widespread (N stands for any base, Y stands for pyrimidine and R stands for purine) (5–16). This observation has raised the question whether GNRA tetraloops other than GYRA and GAAA tetraloops can form equivalent specific long-range interactions. This was addressed, at least partially, when several new receptors for GUAA, GUGA, GAAA and GGAA tetraloops were identified by *in vitro* selection experiments (8,15) and were shown to have thermodynamics and loop selectivity comparable to natural ones when tested in standard physiological conditions (15) (E. C., S. Baudrey, L. J., unpublished data). Most of these *in vitro* selected loop/receptor interactions, including the GAAA/C7.2 (8), GAAA/C7.10 (8), GUAA/B7.8 (8), GGAA/R1 (15) and GGAA/R2 (15) loop/receptors, are not observed in known group I (8,16,17) and group II introns (6,8), RNase P RNAs (9,18), molybdenum cofactor riboswitches (19), class I di-GMP riboswitches (20) and ribosomal RNAs. In order to explain the evolutionary bias toward natural GNRA/receptor interactions versus those obtained by *in vitro* selection, other selection pressures than those for particular biochemical and biophysical properties should be at work during the structural evolution of natural RNA molecules.

In vitro selected loop/receptor interactions are typically more ‘G/C-rich’ than their natural counterparts. Even naturally occurring GAAA/11 nt receptors, which can accommodate AA, AC and GU dinucleotide platforms, strongly favor the AA platform versus all the others (8,21). This suggests that natural RNA motif sequences might be selected for their robustness toward intra-molecular RNA misfolding rather than for their local thermodynamic stability or selectivity. Natural helical and ‘A/U-rich’ GNRA receptors are more likely to avoid kinetic and

*To whom correspondence should be addressed. Tel: +1 805 893 3628; Fax: +1 805 893 4210; Email: jaeger@chem.ucsb.edu

thermodynamic folding traps at the level of larger sequence contexts than their artificial counterparts. On the other side, 'G/C-rich' receptors might be more suited for designing artificial riboswitches able to attenuate formation of GNRA/receptor interactions.

Previously, we developed a self-assembling tectoRNA heterodimer system based on bimolecular GNRA/receptor interactions that was employed as building blocks for nano-constructions (3,15,22–27) and *in vitro* selection of novel GGAA receptors (15) (Figure 1). Inspired by working principles from natural transcription attenuators (28–31), we have engineered several tectoRNA riboswitches able to adopt mutually exclusive structures that promote or inhibit formation of GNRA/receptor interactions (Figure 1). These tectoRNA riboswitches are used to monitor the ability of several tetraloop/receptor motifs with different G/C content to be thermodynamically trapped by pseudoknot (PK) formation. The mechanism of attenuation of inter-molecular GNRA/receptor interactions by intra-molecular PK is investigated

by gel-shift assays, lead cleavage probing, competition experiments and co-transcriptional assembly assays. While our data shed new light on the structural evolution of GNRA/receptor interactions, it also provides new design principles for RNA-based switching devices suitable for synthetic biology and nanobiotechnology (32–34).

MATERIALS AND METHODS

TectoRNA design and 3D modeling

3D atomic models were manually constructed using the program Swiss-Pdb Viewer (35) following the RNA architectonics guidelines (24). All tectoRNA attenuators contain a heterodimer-forming module that assembles with a probe through two inter-molecular receptor/GNRA interactions (Figures 1 and 2). This module was modeled after the tectoRNA heterodimer (HD) (15,22,23) for which atomic model structures are presently available [PDB_ID: 2adt] (36,37). The 5' and 3' PK forming modules leading to the formation of 5' and 3'

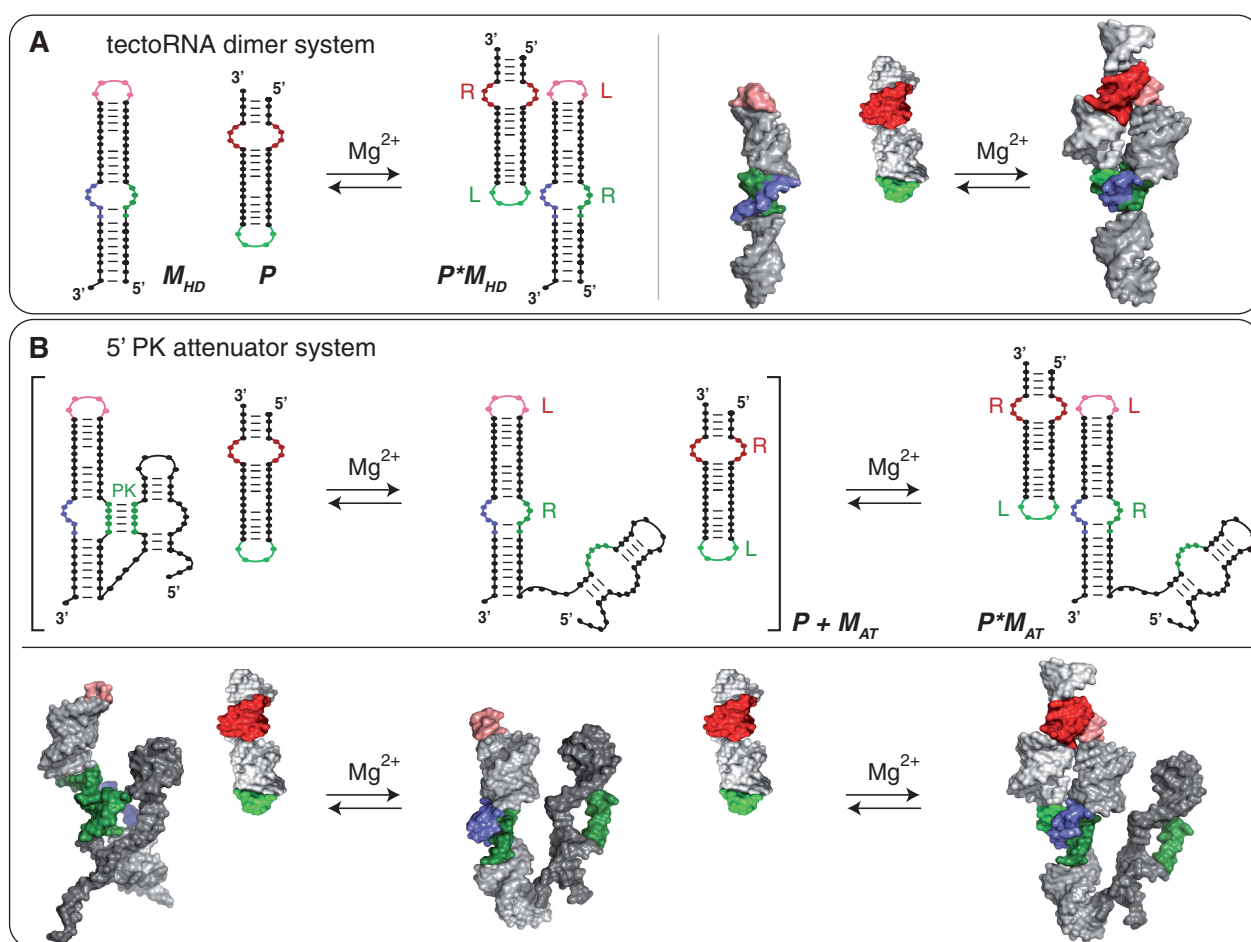


Figure 1. Self-assembly equilibrium reactions for the tectoRNA systems reported. **(A)** TectoRNA heterodimer (HD) system: a HD-forming module (M_{HD}) assembles with a probe (P) through GNRA/receptor interactions to form a heterodimer ($P \times M_{HD}$). This system is used as control. **(B)** 5' PK attenuator system: the tectoRNA attenuator (M_{AT}), consisting of a HD-forming module linked to a PK-forming module, can assemble with a probe (P) through its HD-forming module (equilibrium on the right) to form the heterodimer ($P \times M_{AT}$). Attenuation of inter-molecular self-assembly between the tectoRNA attenuator and the probe occurs when the PK-forming module interacts with the 5' side (in green) of the receptor of the HD-forming module to form a 5' PK (equilibrium reaction between brackets). Interacting receptor (R) and loop (L) motifs as well as pseudoknot (PK) are indicated. Equilibrium reactions and 3D stereo view for the 3' PK attenuator system are provided Supplementary Figure S1.

tested, the K_d 's equation is: $K_d = [(M_0)(1-f)^2]/f$. Therefore, K_d 's correspond to $M_0/2$ when 50% of bi-molecular assemblies are formed (15,23). For each set of molecules, K_d values correspond to the average calculated from three independent experiments. The corresponding free energy variations of dimerization (ΔG_{HD}) between tectoRNA attenuators and cognate RNA probes are determined from the equation, $\Delta G_{HD} = RT \ln K_d$, where R is the gas constant (1.985 cal/K/mol) and T is the temperature (283°K). The apparent free energy variation of attenuation at 10°C ($\Delta \Delta G_{AT}$) can be derived from the equation, $\Delta \Delta G_{AT} = \Delta G_{HD}(M_{AT} + P) - \Delta G_{HD}(M_{HD} + P)$, where, $\Delta G_{HD}(M_{AT} + P)$ is the free energy of dimerization between the tectoRNA attenuator (comprising attenuator PK-forming and HD-forming modules) and its cognate RNA probe, and $\Delta G_{HD}(M_{HD} + P)$ is the free energy variation of dimerization between the corresponding HD-forming module alone and its cognate probe. All K_d 's and associated ΔG_{HD} and $\Delta \Delta G_{AT}$ are reported in Supplementary Tables S2–S4.

Co-transcriptional assembly

PCR-generated DNA templates coding for a tectoRNA attenuator and its cognate RNA probe (GAAA2 or GGAA2; Supplementary Table S1) were mixed at equimolar concentrations in presence of the transcription mixture [50 mM Tris pH 7.5, 10 mM MgCl₂, 2 mM spermidine, 2.5 mM NTPs, 10 mM DTT, α [³²P]-ATP (10 mCi/ml)]. Transcription was initiated by addition of home-made T7 RNA polymerase (10 U/ μ l final) at 37°C. Small aliquots of the transcription mix were taken at 15-, 30-, 45- and 60-min time intervals and quenched by incubation with RQ1 RNase-free DNase (0.3 U/ μ l final) for 15 min at 37°C, just before native PAGE analysis at 10°C in presence of 10 mM Mg(OAc)₂ as described above.

Lead Pb(II)-induced cleavage

RNA samples (4 μ M final with 10 nM of 3'-end labeled RNA) assembled as described above, were incubated in presence of Pb(OAc)₂ (8 mM final) for 2 min before addition of 50 mM EDTA and ethanol precipitation (15,23). Lead-induced cleavage patterns were visualized on 8 M Urea/20% PAGE (see also Supplementary Data). Cleaved positions were identified using RNA samples treated by RNase T1 digestion and alkaline hydrolysis.

RESULTS

Modular design of tectoRNA attenuators

Each tectoRNA attenuator contains a 'pseudoknot (PK)-forming' module linked in 5' to a 'heterodimer (HD)-forming' module (Figure 1 and Supplementary Figure S1). The 'HD-forming' module is based on a previous self-dimerizing tectoRNA construct (15,22,23) that consists of a GNRA receptor tectoRNA unit assembling through bimolecular GNRA/receptor interactions with a

tectoRNA probe (Figures 1 and 2). Because of the high recognition specificity of GAAA and GGAA tetraloops by their cognate receptors, HD-forming modules cannot self-assemble in the absence of probe. The 'PK-forming' module contains an internal loop called the PK-forming loop (or PKL) and promotes formation of an intra-molecular PK with the 5' or 3' side of the receptor from the 'HD-forming' module. This PK competitively inhibits assembly with the GRAA probe (Figure 1). In other words, pseudoknot formation attenuates tectoRNA dimer formation. While tectoRNA attenuators are based on the same structural scaffold, they essentially differ from one another at the level of their receptor and PKL sequences (Figures 2 and 3C, Supplementary Table S1). We designed a total of 17 different attenuators (numbered 1–17) by combining five HD-forming modules based on the 11nt and R1 receptor sequences (11nt_AA, 11nt_AC, 11nt_GU and 11nt_A/CC) (8,15), with various PK-forming modules containing different PKL loop sequences (3'KL_AA, 3'KL_AC, 3'KL_GU, 5'KL, 5'KL_A/CC and 5'KL_R1), with up to 5 to 6 nt complementary to the 3' or 5' sides of the receptor. The resulting intra-molecular PKs are structurally and conceptually similar to the binding modality of stable inter-molecular paranemic RNA molecules previously shown to require a minimum of 5 bps for self-assembly (46). The effects of additional nucleotide variations were investigated within the context of some of these constructs (Supplementary Table S1). To check the influence of PKL size on PK formation, two additional adenines were introduced in the PKL, on the strand opposite to the PK forming strand (Molecules of the 1a–17a series). To modulate the binding affinity of the HD-forming module for its cognate probe, the gGRAAU terminal loop of the HD-forming module was changed into a gGRAAc loop (Molecules of the 1''–17'' and 1a''–17a'' series).

Characterization of tectoRNA attenuators based on GAAA/11 nt receptor interactions

Free energies of dimerization (ΔG_{HD}) between HD-forming modules and their cognate probe can be derived from equilibrium constants of dissociation estimated by native PAGE gel-shift assays as indicated in the Materials and Methods section (Figure 3A and B, Supplementary Table S2). By comparing ΔG_{HD} of a particular HD-forming module in the tectoRNA attenuator context with the one in absence of linked PK-forming module, we can estimate for each tectoRNA attenuator the variation of free energy ($\Delta \Delta G_{AT}$) that corresponds to attenuation by PK formation (see Materials and Methods section).

At 15 mM Mg(OAc)₂ and 10°C, most HD-forming modules based on the 11nt receptor variants (Supplementary Figure S2) assemble to the GAAA probe with very similar ΔG_{HD} . ΔG_{HD} 's for the 11nt_AA, 11nt_AC and 11nt_GU modules are almost undistinguishable (see HD_1, HD_4 and HD_7 in Supplementary Table S2) while the 11nt_A/CC receptor, which differs by three point mutations from the classic

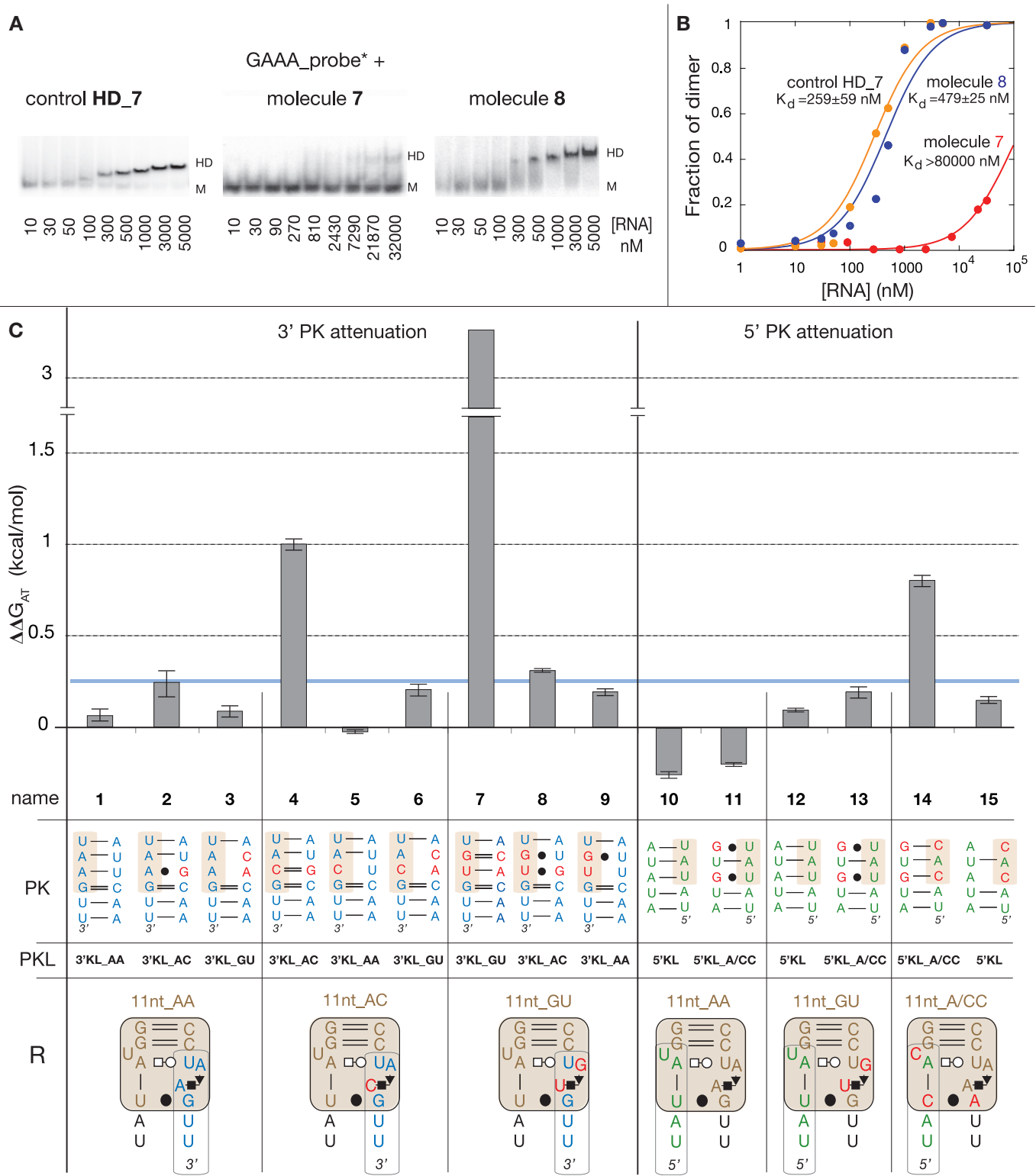


Figure 3. Thermodynamic analysis of tectoRNA attenuators based on 11 nt receptor variants. (A) Typical examples of native PAGE titration experiments at 15 mM Mg(OAc)₂ and 10°C, for the control DF_7 (11nt_GU HD-forming module alone), molecule 7 (11nt_GU HD-forming and 3'KL_GU PK-forming modules) and molecule 8 (11nt_GU HD-forming and 3'KL_AC PK-forming modules) in presence of equimolar concentrations of radiolabeled GAAA probe. M and HD indicate the position of monomers and heterodimers, respectively. (B) Titration curves with calculated equilibrium constants of dissociation (K_d 's) corresponding to the tectoRNA assemblies in (A). (C) Free energies of attenuation of heterodimer formation for all attenuator constructs based on the 11 nt receptor variants (see also Supplementary Table S3). The free energies of attenuation ($\Delta\Delta G_{AT}$) were estimated at 10°C and 15 mM Mg(OAc)₂ as described in the Materials and Methods section. The sequence of the intra-molecular 3' or 5' PK, which competes with heterodimer formation by sequestering either the receptor 3' or 5' side, the name of the PK-forming module (PKL) and the 2D structure and name of the receptor (R) from the HD-forming module are indicated for each tectoRNA attenuator tested (numbered 1–15). All constructs with $\Delta\Delta G$ values below the threshold of 0.25 kcal/mol (indicated by the blue line) are considered to have no significant attenuation. This threshold was estimated based on the range of standard error deviations observed through the study (Supplementary Table S1).

11nt_AA receptor, leads to a minor decrease of 0.43 kcal/mol in binding affinity when compared to the 11nt_AA receptor (**HD_14** in Supplementary Table S2). Overall, this result corroborates the isosteric nature of the AA, GU and AC dinucleotides platforms, which structurally contribute in a similar way to the stabilization of the GAAA tetraloop/11nt receptor interaction within the HD-forming module context.

In contrast, some of the tectoRNA attenuators based on these receptors display markedly different behaviors (Figure 3). Attenuators **1**, **4** and **7** have PK-forming modules designed to form a PK of 6 WC bps with the 3' sides of receptors 11nt_AA, 11nt_AC and 11nt_GU, respectively. While no significant change in binding affinity is observed for molecule **1** with respect of **HD_1**, molecules **4** and **7** attenuate heterodimer formation by 1 and 3.3 kcal/mol, respectively. Other 3'PK attenuators with combinations of HD-forming and PK-forming modules that introduce G:U bp and/or WC mismatches in the PK do not present significant attenuation (molecules **2**, **3**, **5**, **6**, **8** and **9**). This data suggests that attenuation is correlated to the stability of the PK that requires at least two G:C bps to efficiently compete with heterodimer formation. Similar results are provided by 5'PK attenuators **10**, **12** and **14**, designed to form pairings of 5 WC bps with the 5' sides of receptors 11nt_AA, 11nt_AC and 11nt_GU, respectively. Molecules **10** and **12** are unable to trap the receptors but molecule **14**, which can form a PK with 2 G:C bps, attenuates heterodimer formation by 0.80 kcal/mol (Figure 3). Not surprisingly, none of the attenuator combinations with PKs with G:U or A:C bps are able to compete with heterodimer formation.

Additional structural evidences for intra-molecular PK formation in attenuator **7** are provided by lead cleavage experiments (Figure 4 and Supplementary Figure S3). Lead is widely used as a conformational probe for RNA because it preferentially cleaves the phosphodiester backbone in flexible regions or non-canonically paired motifs of RNA molecules (15,22,23,25,46). Irrespective from absence or presence of the GAAA probe, the 3' strand of the 11nt_GU receptor of attenuator **7** is strongly protected toward cleavage in comparison to the one of molecules **8** (or **9**). Additionally, the 5' PK strand within the PK-forming module of **7** also shows enhanced protection toward lead cleavage relative to **8** (or **9**). This strongly suggests that the PK is formed in attenuator **7** but not in **8** (or **9**). In contrast, in presence of the GAAA probe, molecules **8** and **9** display partial protection of the receptor and tetraloop regions from the HD-forming module, corroborating their assembly with the probe.

In summary, the 11nt receptor can easily accommodate sequence variations that are all able to efficiently promote self-assembly with the cognate GAAA tetraloop. However, the ability to trap its sequence in an alternative conformation like a PK, is highly dependent of the presence of Gs or Cs, G:C bps being much more effective than U:A bps for stabilizing alternative WC pairings.

Modulating tectoRNA attenuation with an artificial receptor, point mutations and magnesium

The GGAA/R1 receptor interaction was isolated by *in vitro* selection (15). It is highly selective for the GGAA tetraloop and its affinity is comparable to GAAA/11 nt receptor interactions (15). Interestingly, R1 is four mutations away from the 11nt_AA receptor but only two mutations away from the 11nt_GU with which it shares an identical 3'-side (Figure 5A). R1 is, however, more 'G/C-rich' than any of the 11nt variants. Consequently, the resulting attenuators **16** and **17** are expected to form stable intra-molecular 3' and 5' PKs, respectively: according to Freier's (47) table, the calculated stability of the 3'PK of **16** and 5'PK of **17** is -5.3 and -3.5 kcal/mol, respectively. As shown in Figure 5B, molecules **16** and **17** attenuate heterodimer formation with their cognate GGAA probe by 2.16 and 1.91 kcal/mol, respectively. While both molecules **7** and **16** form the same 3'PK, attenuation with **16** is less dramatic than with **7** in presence of their respective probes; this could be explained by the fact that the **HD_16** heterodimer complex involving the GGAA/R1 interaction, is 0.5 kcal/mol more stable than the **HD_7** heterodimer complex involving the GAAA/11nt_GU interaction (Supplementary Table S2). Therefore, for **16**, heterodimer formation is advantaged with respect of PK formation.

TectoRNA heterodimer assembly, which occurs through two GNRA/receptor interactions, is favored by a point mutation that changes the gGRAAU terminal loop of the HD-forming module into a gGRAAc loop. The thermodynamic stability of the resulting HD heterodimers is increased by 0.5–1.2 kcal/mol at 10°C and 15 mM Mg(OAc)₂ (Supplementary Table S3). This is likely due to small structural variations that favor the local stabilization of gGRAAc/receptor interactions versus gGRAAU/receptor interactions. When incorporated within attenuators **7**, **16** and **17** (to give **7''**, **16''** and **17''**), this mutation leads to a reduction of attenuation by 2- to 5-fold (Figure 5B).

TectoRNA assembly is particularly sensitive to small variations in magnesium concentration (3,22,23). By reducing magnesium concentration from 15 to 2 mM, the affinity between heterodimer modules and corresponding probes decreases by 1.5–2 kcal/mol (Supplementary Table S4). Intra-molecular formation of 3' or 5' PK, which relies on the formation of canonical WC bps, should not be as sensitive to magnesium as inter-molecular formation of GNRA/receptor interactions. As expected, molecule **7''** and to a lesser extent, molecules **17''** and **16''**, attenuate HD formation more effectively at 2 mM than at 15 mM magnesium (Figure 5B).

TectoRNA attenuators of the **1a–17a** series, with two additional adenines in their PKL, were also tested in order to determine whether the size of the PKL could affect PK formation in conjunction with the nucleotide composition of the PK. The behavior of the **1a–17a** attenuator series is overall comparable to the one of the **1–17** attenuator series (Figure 5 and Supplementary Figure S4). At 15 mM magnesium, a small enhancement of attenuation is noticeable

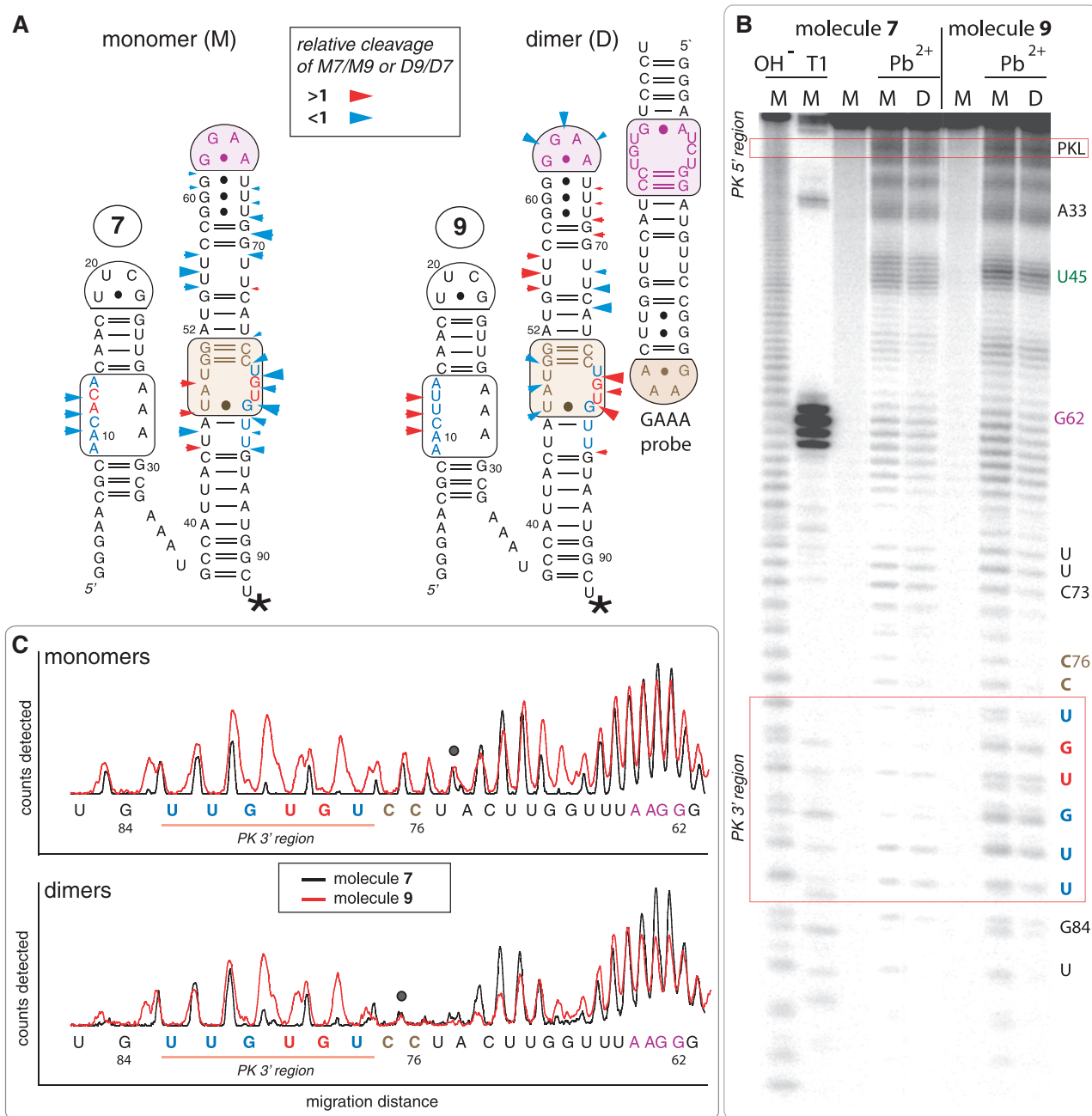


Figure 4. Lead(II)-induced cleavage patterns for tectoRNA attenuators 7 and 9 in their monomeric and heterodimeric states. (A) 2D diagrams of tectoRNA attenuators with reported differential Pb(II) cleavage patterns in the monomeric (M) and heterodimeric (D) states. Phosphate positions in monomer 7 (M7) that show enhanced or reduced Pb(II) cleavage with respect to monomer 9 (M9) are indicated by red or blue arrows on the 2D diagram of 7, respectively. Phosphate positions in heterodimer 9 (D9) that show enhanced or reduced Pb(II) cleavage with respect to heterodimer 7 (D7) are indicated by red or blue arrows on the 2D diagram of 9, respectively. The size of the arrows is roughly proportionate to the difference in cleavage for M7 versus M9 or D9 versus D7. A star indicates the radiolabeled RNA 3'-end. (B) Pb(II) cleavage patterns of ³²P radiolabeled molecules 7 and 9 either alone or bound to their non-radioactive cognate GAAA probe [as shown in (A)]. M and D correspond to monomer and dimer lanes, respectively. Cleavage experiments (indicated by Pb²⁺) were carried out as described in the Materials and Methods section; OH⁻ indicates alkaline hydrolysis ladder; T1 indicates RNase T1 digestion. (C) Superposed lead cleavage profiles for monomers 7 and 9 (top) and for the corresponding heterodimers in presence of GAAA probe (bottom). Black dots indicate positions used for normalization. Similar results are obtained by comparing attenuators 7 and 8 (Supplementary Figure S3).

for molecules **1a**, **10a** and **12a** versus **1**, **10** and **12**. This indicates that 'A/U-rich' PKs form better when the size of PKL is increased, probably because of less steric hindrance.

In summary, these results indicate that the most effective tectoRNA attenuators are those based on 'G/C-rich' receptors such as the R1 and 11 nt-GU receptors. The extent of tectoRNA attenuation can be modulated as a

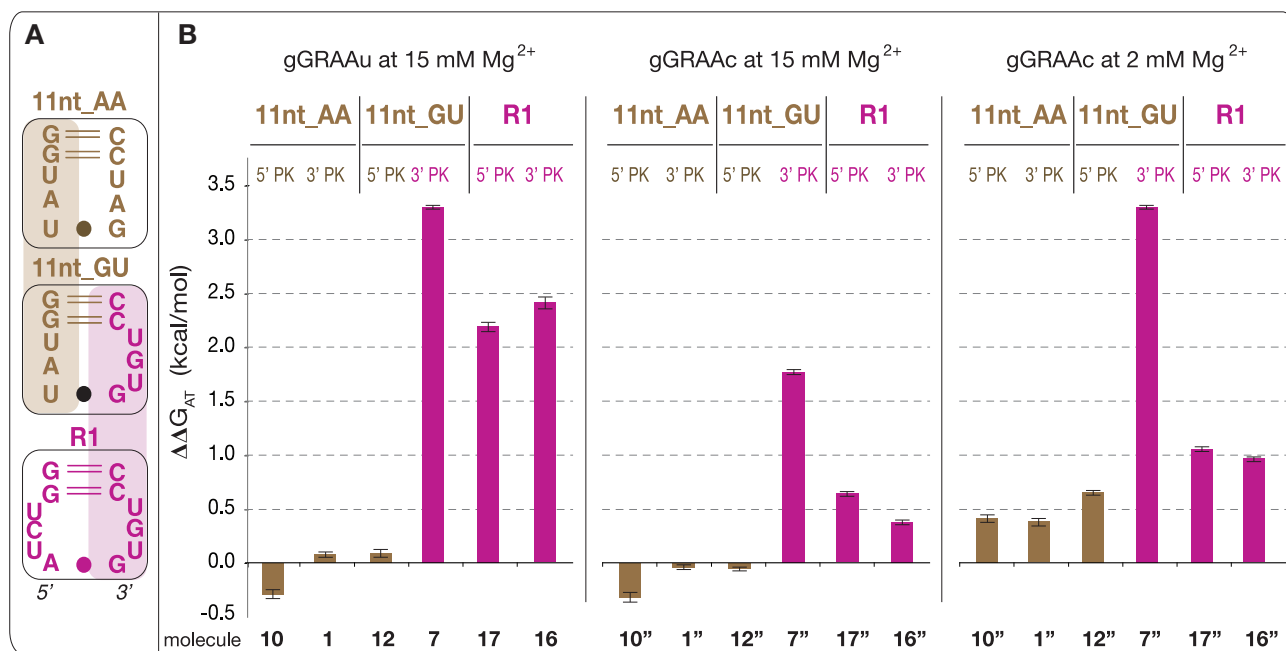


Figure 5. Thermodynamic analysis of tectoRNA attenuators based on the 11 nt and R1 receptors. (A) Sequence relationships between the R1 (15), 11nt_GU [or C7.10 (8,15)] and 11 nt receptors. (B) Free energies of attenuation of heterodimer formation for all attenuator constructs based on the 11 nt and R1 receptors (see also Supplementary Table S4). The free energies of attenuation ($\Delta\Delta G$) were estimated at 10°C and 2 or 15 mM Mg(OAc)₂ as described in the Materials and Methods section. Attenuator molecules 1'', 7'', 10'', 12'', 16'' and 17'' differ from molecules 1, 7, 10, 12, 16 and 17 by the presence of gGRAAc terminal loops (instead of gGRAAU). This single nucleotide variation increases heterodimer stability. A similar series of attenuator constructs with PK-forming loops involving five As (instead of three) show similar attenuation results (Supplementary Figure S4).

function of magnesium concentration as well as peripheral single point mutations in a predictable manner. From a rational design point of view, our results suggest that artificial 'G/C-rich' receptors are better suited than 'A/U-rich' receptors for designing riboswitches that require folding into alternative RNA structures. However, from an evolutionary point of view, 'G/C-rich' receptors might be disadvantageous because they are more prone to trap native RNA sequences into alternative undesirable structures.

TectoRNA attenuation during *in vitro* transcription

We have also investigated how tectoRNA attenuation could occur during *in vitro* RNA transcription in isothermal conditions (37°C) (see 'Materials and Methods' section). While all the experiments described above were performed in conditions usually favoring thermodynamic control versus kinetic control, co-transcriptional assembly experiments should be more representative of folding and assembly processes taking place within the cell (48,49). During the linear phase of RNA transcription, three different types of products are observed on native PAGE: the RNA probe, the tectoRNA attenuator and the complex resulting from the inter-molecular assembly between the probe and attenuator molecules (Figure 6A and Supplementary Figure S5). Because of its smaller size, the probe product is transcribed in larger quantity than the attenuator product, explaining why a portion of it always remains unassembled. In presence of GAAA probe, the totality of attenuator 1 (and 10) products assembles to the probe (Figure 6B). In contrast, only ~60%

of the attenuator 4 product forms a stable complex with the probe, suggesting that the remaining 40% is blocked into the PK conformation state (Figure 6B). In perfect agreement with previous data, attenuator 7 (and 7'') demonstrates full attenuation of tectoRNA assembly, while attenuator 9, which differs from molecule 7 by only two point mutations within its intra-molecular PK, assembles with the probe to its full extent (Figure 6B and Supplementary Figure S5). Interestingly, attenuators 14, 16 and 17 assemble with their cognate probe to form complexes with faster gel mobility than those obtained with attenuator 1, 9 and 10 (Supplementary Figure S5). We have observed that tectoRNA complexes with higher K_d 's (or lower affinities) typically migrate faster at lower RNA concentrations than those with lower K_d 's (or higher affinities) (15,23). This behavior has been described as resulting from monomers and heterodimers being in dynamic equilibrium (15,23). Our observation corroborates the fact that attenuators 14, 16 and 17 bind less efficiently their cognate probe than their corresponding HD_forming modules. In these attenuators, formation of a transient intra-molecular PK likely displaces the inter-molecular assembly equilibrium toward the monomers.

Overall, co-transcriptional assembly data corroborate those obtained previously. To effectively attenuate tectoRNA assembly, the 3' and 5' PK base pairings need to have a calculated thermodynamic stability lower than -4 and -3 kcal/mol, respectively. Co-transcriptional data also suggest that attenuation can occur through two

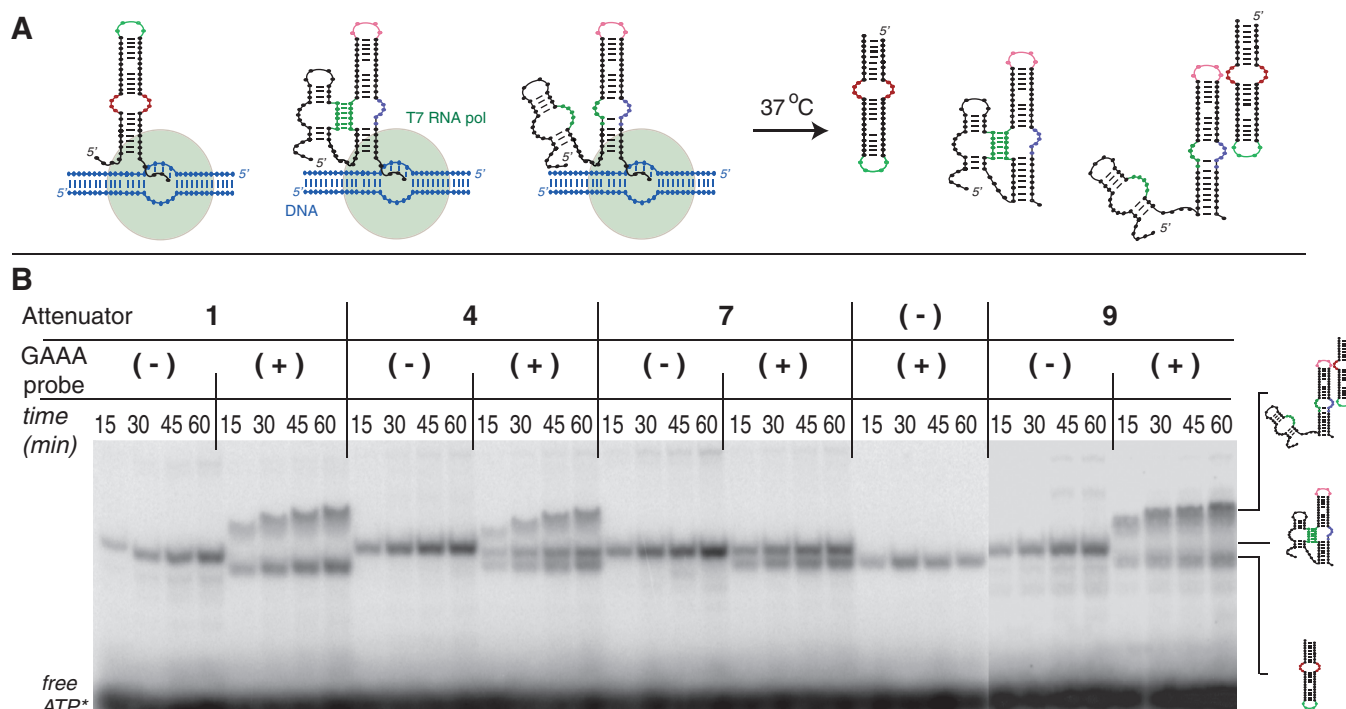


Figure 6. Co-transcriptional assemblies of tectoRNA attenuators **1**, **4**, **7** and **9** in presence (or absence) of cognate GAAA probe. (A) Schematic illustrating the possible molecular states adopted by the tectoRNA attenuator system during its transcription from DNA templates (in blue) by T7 RNA polymerase (in green) at 37°C in presence of 10mM Mg²⁺. (B) Native PAGE analysis of different tectoRNA attenuator transcription mixtures at various times in presence (+) or absence (-) of GAAA probe: co-transcriptional assembly is monitored by RNA body-labeling with α [P³²]ATP and native PAGE is performed at 10°C and 10mM Mg(OAc)₂ after quenching the transcription with DNase as described in the 'Materials and Methods' section. See also Supplementary Figure S5.

distinct mechanisms. In the mechanism shared by attenuators **4**, **7** and **7''**, the attenuator RNA product folds into stable PK_ forming and HD_ forming conformers, which are unable to interchange into one another. This is probably due to the PK_ forming conformer acting as a folding trap, unable to switch into the HD_ conformer. In the second mechanism shared by attenuator **14**, **16** and **17**, the PK_ forming and HD_ forming conformers are in dynamical equilibrium with one another, allowing the PK_ forming conformer to switch into the HD_ forming conformer. In the future, further work will be needed to unravel the dynamical and structural constraints favoring one mechanism versus the other.

Controlling tectoRNA attenuation with small RNA switches

Moving toward more complex tectoRNA attenuator devices, we designed a tri-molecular system aiming at controlling tectoRNA attenuation with small RNA inhibitors acting as molecular switches (Figure 7A). TectoRNA attenuator **18** is derived from attenuator **7**, from which it differs by four point mutations in the PKL, on the strand opposite to the PK forming sequence (Figure 7B). Two small RNAs, **SW(I)** and **SW(II)**, are designed to favor heterodimer formation between **18** and the GAAA probe by preventing intra-molecular PK formation (Figure 7A): they assemble to the PK-forming loop according to two equivalent structural modalities expected to perfectly mimic the assembly of the U65 ψ pocket

(U65hp) of human U65 H/ACA snoRNA with its rRNA substrate (38,39) (Figure 7B). In presence of the GAAA probe, attenuator **18** has a more modest attenuation potential than attenuator **7** (-0.84 kcal/mol versus -3.24 kcal/mol): this possibly results from the formation of additional non-canonical bps, which might stabilize the internal structure of the PKL of **18** and disfavor PK formation. Nevertheless, when either **SW(I)** or **SW(II)** are added to the mix, the affinity of **18** for the GAAA probe significantly increases to be similar to the one observed for the HD_7:GAAA probe complex (~0.2 kcal/mol). Molecules **SW(I)** and **SW(II)** bind to the PK_ forming module of **18** with K_d 's of 7.3 and 16.8 nM, respectively. While these values are consistent with previously published results for similar binding interactions (46), they indicate that **SW(I)** and **SW(II)** can completely switch off the PK_ forming module of **18** and prevent the formation of the intra-molecular 3'/PK with the 11nt_GU receptor of the HD_ forming module. Therefore, these results provide further evidence in support of the mechanism of attenuation of heterodimer formation through intra-molecular PK formation.

DISCUSSION

Implications for the rational design of RNA 3D structures

Using a rationally designed molecular system based on tectoRNA self-assembly, we have demonstrated that the formation of GNRA/receptor tertiary interactions can be

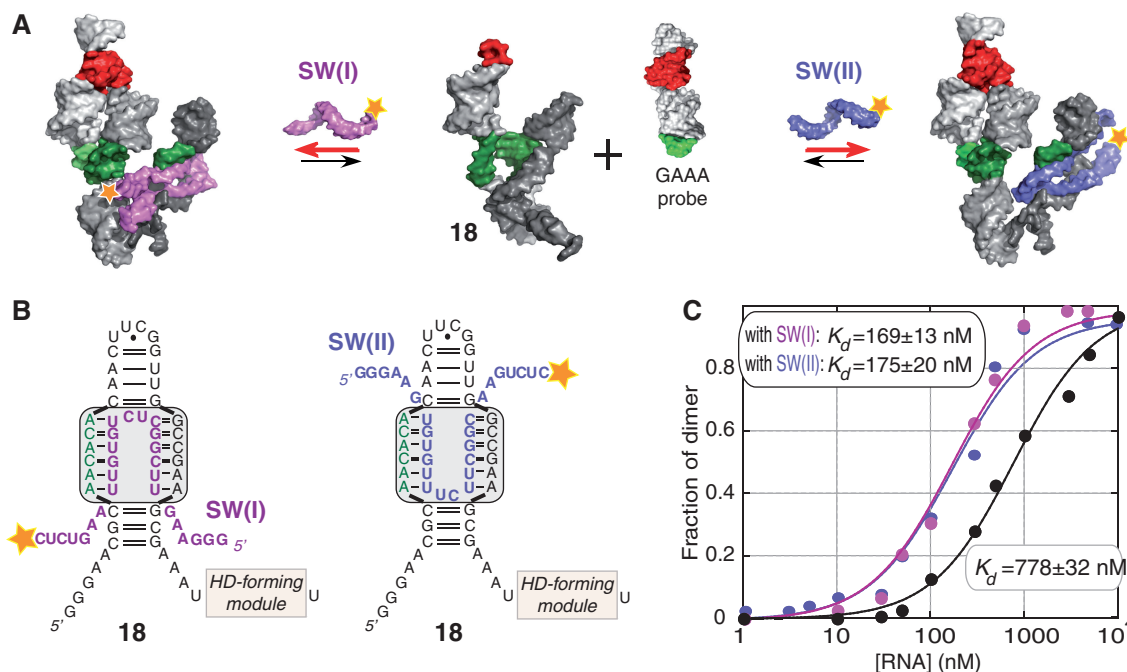


Figure 7. Switching off a tectoRNA attenuator with small RNA oligonucleotides. (A) Schematic of the self-assembly equilibrium reaction of tectoRNA attenuator **18** in presence of two small RNAs [SW(I) and SW(II)] that favor heterodimer formation by preventing internal PK formation. The two small RNAs switch off the PK attenuator module by assembling to the PK-forming loop in a way expected to perfectly mimic the NMR structures of the pseudouridylation pocket of the Box H/ACA snoRNA bound to its rRNA substrate [PDB codes: 2p89 (38) and 2pcv (39)]. (B) 2D structure diagrams of the PK-forming module of attenuator **18**, bound to SW(I) and SW(II) small switching RNAs. Two possible equivalent binding modalities (boxed in grey) are shown. (C) Titration curves with calculated equilibrium constants of dissociation (K_d 's) corresponding to the assembly of attenuator **18** with the GAAA probe in absence (black circles) or presence of switching RNAs [magenta circles for SW(I) and blue circles for SW(II)]. Experiments were carried out at 15 mM Mg(OAc)₂ and 10°C as described in the 'Materials and Methods' section.

attenuated by formation of alternative PK structures: the higher the G/C content of the sequence signature of the GNRA receptor motif, the more easily this sequence can be trapped into an alternative pseudoknot structure that attenuates its ability to recognize a GNRA loop target. From a rational design point of view, these data make perfect sense because 'G/C-rich' base pairings are thermodynamically more stable than 'U/A-rich' base pairings. However, the data also highlight that it is a rather narrow thermodynamic threshold that determines whether the PK can effectively attenuate the formation of GNRA/receptor interactions *in vitro*. For instance, only one additional C or G in the nucleotide platform of the 11 nt motif (11nt_GU and 11nt_AC versus 11nt_AA) is sufficient for stabilizing by 1.5–2 kcal/mol the resulting PKs and lead to attenuation. Nevertheless, if most PKs (with at least one G:C bp) were accurately predicted with the Kinefold program (42), the overall quantitative extent of attenuation cannot yet be predicted from purely theoretical thermodynamic analysis. Indeed, our tectoRNA attenuation system depends on the thermodynamic stability of RNA tertiary interactions and structure motifs that essentially involve non-canonical bp interactions and that are also very sensitive to divalent ion concentration. *In vitro* cotranscriptional self-assembly revealed that attenuation could proceed in isothermal conditions according to two mechanisms that could be distinguished based on whether the PK-forming and the HD-forming conformers are in dynamical equilibrium or not. Previous

studies (48,49) have shown that kinetics and thermodynamics make different contributions to RNA folding *in vitro* and *in vivo*: it is therefore possible that the exchange between stable alternative tertiary structures might be more rapid *in vivo* than *in vitro* (48,49). Clearly, further work will be necessary to understand tectoRNA attenuation mechanisms in more detail, especially within the context of cells. In any case, our data already provide RNA modules and design principles that can be used for developing controllable artificial RNA nano-switches with tunable binding properties for nanobiotechnology and synthetic biology applications. For instance, we have demonstrated that RNA tertiary interactions can be specific target locations for designing RNA switches that allow precise modulation of the folding and assembly of these RNA molecules. Because of the large number of topologically equivalent GNRA/receptor interactions presently available (8,14,15), these interactions offer high structure designability for the rational design of RNA nanodevices (27). The choice of a particular RNA self-assembling motif can vary depending on the intended design goal. A/U-rich RNA motifs can maximize a unique folding pathway by minimizing undesirable folding traps resulting from the formation of alternative bps. Alternatively, G/C-rich tertiary motifs with one or two Gs (or Cs) localized on the same strand, can be used to design artificial RNAs with distinct alternative conformational states. Pseudoknots involving 5–6 bps with two G:C bps are sufficient for

competing with the formation of GNRA/receptor interactions. However, as a difference of a few kcal can displace the equilibrium toward a unique molecular state, a good empirical understanding of the energetic balance between the thermodynamic strength of competing tertiary interactions is necessary for designing truly tunable devices.

Implications for RNA structural evolution

More importantly, our data provide possible clues for RNA structural evolution as they can explain the existence of particular sequence patterns coding for RNA tertiary interactions. GNRA mediated interactions in stable RNAs are essentially dominated by two families: GYRA/helix and GAAA/receptor interactions. For example, in the class I di-GMP riboswitches (20,50,51), ~35% are GYRA/helix motifs and 65% are GAAA/11 nt-like receptor motifs (Supplementary Table S5A). Within the GAAA/11 nt-like receptors, 64% have no more than one G or C, 24% have two G or C and only 12.3% have three G or C or more (Supplementary Table S5B). Therefore, in the 11 nt receptor family, 'U/A-rich' rather than 'G/C-rich' nucleotide compositions are favored at the level of the 11 nt internal loop, with AA platforms (70.4%) being more abundant than AC (8.6%) and GU (11.3%) platforms. Interestingly, the thermodynamic stability and GNRA selectivity of the 'G/C-rich' 11 nt receptor variants are not significantly different from those of the more 'A/U-rich' 11 nt receptors (Supplementary Table S2 and Supplementary Figure S6). Moreover, in addition to class I di-GMP riboswitches, several other natural RNA contexts like RNase P RNAs (9,18), group I (16,17) and group II introns (6,8,52), contain GYRA/helix interactions, which are thermodynamically less stable than most 11 nt receptors, in place of GAAA/11 nt motifs. Considering the range of observed riboswitch behaviors in response to the evolutionary need for precise genetic regulation, the sequence of the GNRA/receptor interaction from the di-GMP riboswitch may be tuned so that the riboswitch functions more as a dimmer or rheostat than a binary on/off switch (53).

In natural RNAs, the GAAA tetraloop is universally more abundant than any of the other GNRA loops (54,55) (Supplementary Table S5A). However, the predominance of the GUAA tetraloop over other GYRA and GRRA tetraloops is not consistent and might depend on the molecular and genomic context (54,55). As exemplified for the di-GMP riboswitch of class I, it is particularly striking that <1.5% of the GNRA/receptor interactions take advantage of other GRRA tetraloops (Supplementary Table S5A), while it has been recently demonstrated that artificial GGRA receptors, such as the highly stable and selective R1 and R2 receptors, could be isolated by SELEX (15). In fact, using the RNAmotif software (56), we searched for the R1, R2 and 11nt_GU (C7.10) sequence signatures and did not identify any of them in known natural RNA sequences such as class I di-GMP riboswitch (20), molybdenum cofactor riboswitch (19), group I introns, group II

introns and RNase P RNA sequences from the rfam database (57). While we cannot rule out the possibility that these receptors exist in some genomes, our search already suggests that they are much less common than the 11 nt receptor.

Based on the mere consideration of thermodynamics, kinetics and loop selectivity, it is not obvious to explain the strong bias toward 'A/U-rich' GAAA/receptors or GYRA/helix receptors in natural stable RNAs. Clearly, higher order selection pressures imposed by the larger structural context of natural RNA molecules, the kinetics constraints on the global folding of RNA inside the cell or the possible involvement of additional cellular components are likely at play (58). Based on our present data, the most straightforward explanation is that the preferred occurrence of natural RNA motif sequences stems from an evolutionary adaptation that make them less prone to misfolding and therefore less likely to interfere with the folding of a large RNA sequence (through formation of alternative pairings or interactions with other regions of the RNA sequence). As we have clearly demonstrated that 'G/C-rich' receptors are more likely to be trapped into alternative PK structures than 'A/U-rich' receptors, we propose that, in cells, the natural GYRA/helix and 'A/U-rich' GAAA/11 nt receptor interactions result from two evolutionary strategies that minimize kinetic and thermodynamic folding traps in large RNA structural contexts. The first strategy, best exemplified by the 'classic' GYRA/helix interaction, takes advantage of receptors that use Cs and Gs to maximize the formation of stable local WC helical regions, preventing them to form long-range alternative pairings. The other strategy takes advantage of AU-rich internal loop motifs, like the 11 nt receptor motif, that minimize the formation of stable alternative base pairings. Interestingly, the IC3 receptor motif, a natural GNRA receptor identified in IC3 group I introns (14), can be seen as a mix of both strategies, with Gs and Cs involved in local bps and U and As involved in a small asymmetrical internal loop (14,15).

Recently, Mitra *et al.* (58) proposed that, in group I introns, the greater thermodynamic stability of a native conformation over non-native structures, achieved through selection of strong tertiary interactions, comes at the expense of slower folding to the catalytic conformation due to formation of long lived intermediates. Efficient folding is therefore achieved by balancing the gain in structural stability due to tertiary contact formation with the probability of misfolding due to loss of conformational freedom. As such, in contrast to other strong but G/C-rich GNRA/receptor interactions selected *in vitro* (8,15), the GAAA/11 nt motif offers a unique sequence pattern with great thermodynamic strength and lower probability to create stable alternative structures.

In conclusion, when a structural motif is part of a large structural network, the avoidance of alternative folding traps could be a significant selective advantage during evolution. We have therefore an example of how the sequence information of the whole RNA molecule could affect from the top-down the sequence information of the small local structural part (59). Similar to the usage of codons in cells, many synonymous RNA structural motifs exist but they

are not identical after all (60). A good understanding of the structural designability of RNA motifs is therefore key for RNA architectonics (3,24,44,61,62) and the future development of RNA synthetic biology and nanobiotechnology, especially when artificial RNA molecules need to operate *in vivo*.

SUPPLEMENTARY DATA

Supplementary Data are available at NAR Online: Supplementary Tables 1–5, Supplementary Figures 1–6 and Supplementary References (63,64).

ACKNOWLEDGEMENTS

L.J. wishes to dedicate this article to Professor Jérôme Lejeune. We wish to thank Dr Namhee Kim for her technical help in the RNA motif search. K.A. and L.J. designed research; K.A. and Y.-P.L. performed biochemical and biophysical experiments; E.C. performed sequence comparative analysis and search; K.A., Y.-P.L. and L.J. analyzed data; K.A. and L.J. wrote the article.

FUNDING

This work was funded by the National Institutes of Health (R01-GM079604 to L.J.). Funding for open access charge: The open access publication charge for this paper has been waived by Oxford University Press—*NAR* Editorial Board members are entitled to one free paper per year in recognition of their work on behalf of the journal.

Conflict of interest statement. None declared.

REFERENCES

- Tinoco, I. Jr and Bustamante, C. (1999) How RNA folds. *J. Mol. Biol.*, **293**, 271–281.
- Noller, H.F. (2005) RNA structure: reading the ribosome. *Science*, **309**, 1508–1514.
- Geary, C., Chworos, A. and Jaeger, L. (2011) Promoting RNA helical stacking via A-minor junctions. *Nucleic Acids Res.*, **39**, 1066–1080.
- Nissen, P., Ippolito, J.A., Ban, N., Moore, P.B. and Steitz, T.A. (2001) RNA tertiary interactions in the large ribosomal subunit: the A-minor motif. *Proc. Natl. Acad. Sci.*, **98**, 4899–4903.
- Jaeger, L., Michel, F. and Westhof, E. (1994) Involvement of a GNRA tetraloop in long-range RNA tertiary interactions. *J. Mol. Biol.*, **236**, 1271–1276.
- Costa, M. and Michel, F. (1995) Frequent use of the same tertiary motif by self-folding RNAs. *EMBO J.*, **14**, 1276–1285.
- Cate, J.H., Gooding, A.R., Podell, E., Zhou, K., Golden, B.L., Kundrot, C.E., Cech, T.R. and Doudna, J.A. (1996) Crystal structure of a group I ribozyme domain: principles of RNA packing. *Science*, **273**, 1678–1685.
- Costa, M. and Michel, F. (1997) Rules for RNA recognition of GNRA tetraloops deduced by *in vitro* selection: comparison with *in vivo* evolution. *EMBO J.*, **16**, 3289–3302.
- Massire, C., Jaeger, L. and Westhof, E. (1997) Phylogenetic evidence for a new tertiary interaction in bacterial RNase P RNAs. *RNA*, **3**, 553–556.
- Abramovitz, D.L. and Pyle, A.M. (1997) Remarkable morphological variability of a common RNA folding motif: the GNRA tetraloop-receptor interaction. *J. Mol. Biol.*, **266**, 493–506.
- Ban, N., Nissen, P., Hansen, J., Moore, P.B. and Steitz, T.A. (2000) The complete atomic structure of the large ribosomal subunit at 2.4 Å resolution. *Science*, **289**, 905–920.
- Adams, P.L., Stahley, M.R., Gill, M.L., Kosek, A.B., Wang, J. and Strobel, S.A. (2004) Crystal structure of a group I intron splicing intermediate. *RNA*, **10**, 1867–1887.
- Torres-Larios, A., Swinger, K.K., Pan, T. and Mondragon, A. (2006) Structure of ribonuclease P—a universal ribozyme. *Curr. Opin. Struct. Biol.*, **16**, 327–335.
- Ikawa, Y., Naito, D., Aono, N., Shiraishi, H. and Inoue, T. (1999) A conserved motif in group IC3 introns is a new class of GNRA receptor. *Nucleic Acids Res.*, **27**, 1859–1865.
- Geary, C., Baudrey, S. and Jaeger, L. (2008) Comprehensive features of natural and *in vitro* selected GNRA tetraloop-binding receptors. *Nucleic Acids Res.*, **36**, 1138–1152.
- Michel, F. and Westhof, E. (1990) Modelling of the three-dimensional architecture of group I catalytic introns based on comparative sequence analysis. *J. Mol. Biol.*, **216**, 585–610.
- Lehnert, V., Jaeger, L., Michel, F. and Westhof, E. (1996) New loop-loop tertiary interactions in self-splicing introns of subgroup IC and ID: a complete 3D model of the *Tetrahymena thermophila* ribozyme. *Chem. Biol.*, **3**, 993–1009.
- Massire, C., Jaeger, L. and Westhof, E. (1998) Derivation of the three-dimensional architecture of bacterial ribonuclease P RNAs from comparative sequence analysis. *J. Mol. Biol.*, **279**, 773–793.
- Regulski, E.E., Moy, R.H., Weinberg, Z., Barrick, J.E., Yao, Z., Ruzzo, W.L. and Breaker, R.R. (2008) A widespread riboswitch candidate that controls bacterial genes involved in molybdenum cofactor and tungsten cofactor metabolism. *Mol. Microbiol.*, **68**, 918–932.
- Sudarsan, N., Lee, E.R., Weinberg, Z., Moy, R.H., Kim, J.N., Link, K.H. and Breaker, R.R. (2008) Riboswitches in eubacteria sense the second messenger cyclic di-GMP. *Science*, **321**, 411–413.
- Cate, J.H., Gooding, A.R., Podell, E., Zhou, K., Golden, B.L., Szewczak, A.A., Kundrot, C.E., Cech, T.R. and Doudna, J.A. (1996) RNA tertiary structure mediated by adenosine platforms. *Science*, **273**, 1696–1699.
- Jaeger, L. and Leontis, N.B. (2000) TectoRNA: one-dimensional self-assembly through tertiary interactions. *Angew. Chem. Int. Ed. Engl.*, **39**, 2521–2524.
- Jaeger, L., Westhof, E. and Leontis, N.B. (2001) TectoRNA: modular assembly units for the construction of RNA nano-objects. *Nucleic Acids Res.*, **29**, 455–463.
- Jaeger, L. and Chworos, A. (2006) The architectonics of programmable RNA and DNA nanostructures. *Curr. Opin. Struct. Biol.*, **16**, 531–543.
- Afonin, K.A. and Leontis, N.B. (2006) Generating new specific RNA interaction interfaces using C-loops. *J. Am. Chem. Soc.*, **128**, 16131–16137.
- Nasalean, L., Baudrey, S., Leontis, N.B. and Jaeger, L. (2006) Controlling RNA self-assembly to form filaments. *Nucleic Acids Res.*, **34**, 1381–1392.
- Ishikawa, J., Fujita, Y., Maeda, Y., Furuta, H. and Ikawa, Y. (2011) GNRA/receptor interacting modules: versatile modular units for natural and artificial RNA architectures. *Methods*, **54**, 226–238.
- Dawid, A., Cayrol, B. and Isambert, H. (2009) RNA synthetic biology inspired from bacteria: construction of transcription attenuators under antisense regulation. *Phys. Biol.*, **6**, 025007.
- Gutierrez-Preciado, A., Henkin, T.M., Grundy, F.J., Yanofsky, C. and Merino, E. (2009) Biochemical features and functional implications of the RNA-based T-box regulatory mechanism. *Microbiol. Mol. Biol. Rev.*, **73**, 36–61.
- Wachter, A. (2011) Riboswitch-mediated control of gene expression in eukaryotes. *RNA Biol.*, **7**, 67–76.
- Breaker, R.R. (2010) Riboswitches and the RNA World. *Cold Spring Harb. Perspect. Biol.*, November 24 (doi:10.1101/cshperspect.a003566; epub ahead of print).
- Hess, H. and Jaeger, L. (2010) Nanobiotechnology. *Curr. Opin. Biotechnol.*, **21**, 373–375.
- Topp, S. and Gallivan, J.P. (2011) Emerging applications of riboswitches in chemical biology. *ACS Chem. Biol.*, **5**, 139–148.

34. de Las Heras, A., Carreno, C.A., Martinez-Garcia, E. and de Lorenzo, V. (2011) Engineering input/output nodes in prokaryotic regulatory circuits. *FEMS Microbiol. Rev.*, **34**, 842–865.
35. Guex, N. and Peitsch, M.C. (1997) SWISS-MODEL and the Swiss-PdbViewer: an environment for comparative protein modeling. *Electrophoresis*, **18**, 2714–2723.
36. Davis, J.H., Foster, T.R., Tonelli, M. and Butcher, S.E. (2007) Role of metal ions in the tetraloop-receptor complex as analyzed by NMR. *RNA*, **13**, 76–86.
37. Davis, J.H., Tonelli, M., Scott, L.G., Jaeger, L., Williamson, J.R. and Butcher, S.E. (2005) RNA helical packing in solution: NMR structure of a 30 kDa GAAA tetraloop-receptor complex. *J. Mol. Biol.*, **351**, 371–382.
38. Wu, H. and Feigon, J. (2007) H/ACA small nucleolar RNA pseudouridylation pockets bind substrate RNA to form three-way junctions that position the target U for modification. *Proc. Natl Acad. Sci. USA*, **104**, 6655–6660.
39. Jin, H., Loria, J.P. and Moore, P.B. (2007) Solution Structure of an rRNA Substrate Bound to the Pseudouridylation Pocket of a Box H/ACA snoRNA. *Mol. Cell.*, **26**, 205–215.
40. Mathews, D.H., Sabina, J., Zuker, M. and Turner, D.H. (1999) Expanded sequence dependence of thermodynamic parameters improves prediction of RNA secondary structure. *J. Mol. Biol.*, **288**, 911–940.
41. Zuker, M. (2003) Mfold web server for nucleic acid folding and hybridization prediction. *Nucleic Acids Res.*, **31**, 3406–3415.
42. Xayaphoummine, A., Bucher, T. and Isambert, H. (2005) Kinfold web server for RNA/DNA folding path and structure prediction including pseudoknots and knots. *Nucleic Acids Res.*, **33**, W605–W610.
43. Leontis, N.B. and Westhof, E. (2001) Geometric nomenclature and classification of RNA base pairs. *RNA*, **7**, 499–512.
44. Afonin, K.A., Bindewald, E., Yaghoobian, A.J., Voss, N., Jacovetty, E., Shapiro, B.A. and Jaeger, L. (2010) In vitro assembly of cubic RNA-based scaffolds designed in silico. *Nat. Nanotechnol.*, **5**, 676–682.
45. Paillart, J.C., Skripkin, E., Ehresmann, B., Ehresmann, C. and Marquet, R. (1996) A loop-loop 'kissing' complex is the essential part of the dimer linkage of genomic HIV-1 RNA. *Proc. Natl Acad. Sci. USA*, **93**, 5572–5577.
46. Afonin, K.A., Cieply, D.J. and Leontis, N.B. (2008) Specific RNA self-assembly with minimal paranemic motifs. *J. Am. Chem. Soc.*, **130**, 93–102.
47. Freier, S.M., Kierzek, R., Jaeger, J.A., Sugimoto, N., Caruthers, M.H., Neilson, T. and Turner, D.H. (1986) Improved free-energy parameters for predictions of RNA duplex stability. *Proc. Natl Acad. Sci. USA*, **83**, 9373–9377.
48. Mahen, E.M., Harger, J.W., Calderon, E.M. and Fedor, M.J. (2005) Kinetics and thermodynamics make different contributions to RNA folding in vitro and in yeast. *Mol. Cell.*, **19**, 27–37.
49. Mahen, E.M., Watson, P.Y., Cottrell, J.W. and Fedor, M.J. (2010) mRNA secondary structures fold sequentially but exchange rapidly in vivo. *PLoS Biol.*, **8**, e1000307.
50. Smith, K.D., Lipchock, S.V., Ames, T.D., Wang, J., Breaker, R.R. and Strobel, S.A. (2009) Structural basis of ligand binding by a c-di-GMP riboswitch. *Nat. Struct. Mol. Biol.*, **16**, 1218–1223.
51. Kulshina, N., Baird, N.J. and Ferre-D'Amare, A.R. (2009) Recognition of the bacterial second messenger cyclic diguanylate by its cognate riboswitch. *Nat. Struct. Mol. Biol.*, **16**, 1212–1217.
52. Toor, N., Keating, K.S., Fedorova, O., Rajashankar, K., Wang, J. and Pyle, A.M. (2010) Tertiary architecture of the *Oceanobacillus ihenyensis* group II intron. *RNA*, **16**, 57–69.
53. Baird, N.J., Kulshina, N. and Ferre-D'Amare, A.R. (2010) Riboswitch function: flipping the switch or tuning the dimmer? *RNA Biol.*, **7**, 328–332.
54. Prathiba, J. and Malathi, R. (2008) Group I introns and GNRA tetraloops: remnants of 'The RNA world'? *Mol. Biol. Rep.*, **35**, 239–249.
55. Sheehy, J.P., Davis, A.R. and Znosko, B.M. (2010) Thermodynamic characterization of naturally occurring RNA tetraloops. *RNA*, **16**, 417–429.
56. Macke, T.J., Ecker, D.J., Gutell, R.R., Gautheret, D., Case, D.A. and Sampath, R. (2001) RNAMotif, an RNA secondary structure definition and search algorithm. *Nucleic Acids Res.*, **29**, 4724–4735.
57. Gardner, P.P., Daub, J., Tate, J., Moore, B.L., Osuch, I.H., Griffiths-Jones, S., Finn, R.D., Nawrocki, E.P., Kolbe, D.L., Eddy, S.R. *et al.* (2011) Rfam: wikipedia, clans and the 'decimal' release. *Nucleic Acids Res.*, **39**, D141–D145.
58. Mitra, S., Laederach, A., Golden, B.L., Altman, R.B. and Brenowitz, M. (2011) RNA molecules with conserved catalytic cores but variable peripheries fold along unique energetically optimized pathways. *RNA*, **17**, 1589–1603.
59. Jaeger, L. and Calkins, E.R. (2011) Downward causation by information control in micro-organisms. *Interface Focus*, September 29 (doi:10.1098/rsfs.2011.0045; epub ahead of print).
60. Plotkin, J.B. and Kudla, G. (2011) Synonymous but not the same: the causes and consequences of codon bias. *Nat. Rev. Genet.*, **12**, 32–42.
61. Severcan, I., Geary, C., Chworos, A., Voss, N., Jacovetty, E. and Jaeger, L. (2010) A polyhedron made of tRNAs. *Nat. Chem.*, **2**, 772–779.
62. Chworos, A., Severcan, I., Koyfman, A.Y., Weinkam, P., Oroudjev, E., Hansma, H.G. and Jaeger, L. (2004) Building programmable jigsaw puzzles with RNA. *Science*, **306**, 2068–2072.
63. Bindewald, E., Kluth, T. and Shapiro, B.A. (2010) CyloFold: secondary structure prediction including pseudoknots. *Nucleic Acids Res.*, **38**, W368–W372.
64. Jaeger, L., Verzemnieks, E.J. and Geary, C. (2009) The UA_handle: a versatile submotif in stable RNA architectures. *Nucleic Acids Res.*, **37**, 215–230.